

## Supporting Information

### **Self-Triggered Click Reaction in Alzheimer's disease Model: *In Situ* Bifunctional Drug Synthesis Catalyzed by Neurotoxic Copper Accumulated in Amyloid- $\beta$ Plaques**

Zhi Du,<sup>a,b</sup> Dongqin Yu,<sup>a,c</sup> Xiubo Du,<sup>d</sup> Peter Scott,<sup>e</sup> Jinsong Ren,<sup>a</sup> and Xiaogang Qu<sup>\*,a</sup>

<sup>a</sup>Laboratory of Chemical Biology and State Key Laboratory of Rare Earth Resource Utilization, Changchun Institute of Applied Chemistry, Chinese Academy of Sciences, Changchun, Jilin 130022, China.

<sup>b</sup>University of Chinese Academy of Sciences, Beijing, 100039, China.

<sup>c</sup>University of Science and Technology of China, Hefei, Anhui 230029, China.

<sup>d</sup>College of Life Sciences and Oceanography, Shenzhen Key Laboratory of Microbial Genetic Engineering, Shenzhen University, Shenzhen, 518060, China.

<sup>e</sup>Department of Chemistry, University of Warwick, Gibbet Hill Road, Coventry CV4 7AL, UK.

## Materials

All reagents were used without any further purification. Organic solvents were purchased from Beijing Chemical Works. Other chemicals were purchased from Acros Organics, Sigma-Aldrich, or Aladdin. A $\beta$  1-40 was purchased from ChinaPeptides Co., Ltd. mOC78 and Alexa Fluor 555-labeled anti-mouse IgG secondary antibodies were purchased from Abcam (Cambridge, UK). Deionized water was obtained from a Milli-Q system (Millipore, Bedford, MA).

## Characterizations

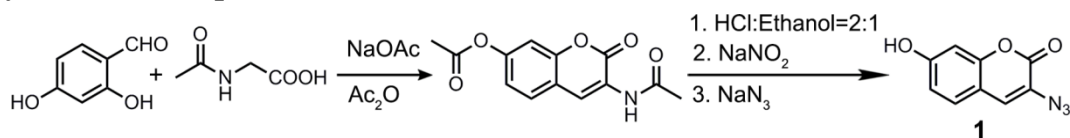
UV-vis spectral measurements were carried out by using a JASCO V-550 UV-Vis spectrophotometer. Fluorescence spectra were measured by a JASCO F-6000 fluorescence spectrometer. Fluorescence microscopy images were obtained using a JASCO FP-6500 spectrofluorometer with the slit width for the excitation and emission of 3 nm.  $^1\text{H}$  NMR spectrum was recorded on a Bruker-600 MHz NMR instrument. Electrospray ionization (ESI) mass spectra (MS) were acquired using the Quattro Premier XE mass spectrometer (Waters, USA). Thermogravimetric analysis was recorded by STA 449 F3 Jupiter simultaneous thermal analyzer.

Atomic force microscopy (AFM) measurements were acquired using a NanoScope V atomic force microscope (Veeco Instruments, Plainview, NY, USA). Isothermal titration calorimetry (ITC) experiments were carried out on a NANO ITC System (TA Instruments Inc., USA). Circular dichroism (CD) spectra were collected with a JASCO J-810 spectropolarimeter. Matrix-assisted laser desorption and ionization time-of-flight mass spectrometry (MALDI-TOF-MS) experiments were carried out on an Autoflex III smartbeam<sup>TM</sup> MALDI-TOF instrument (Bruker, Billerica, MA, USA).

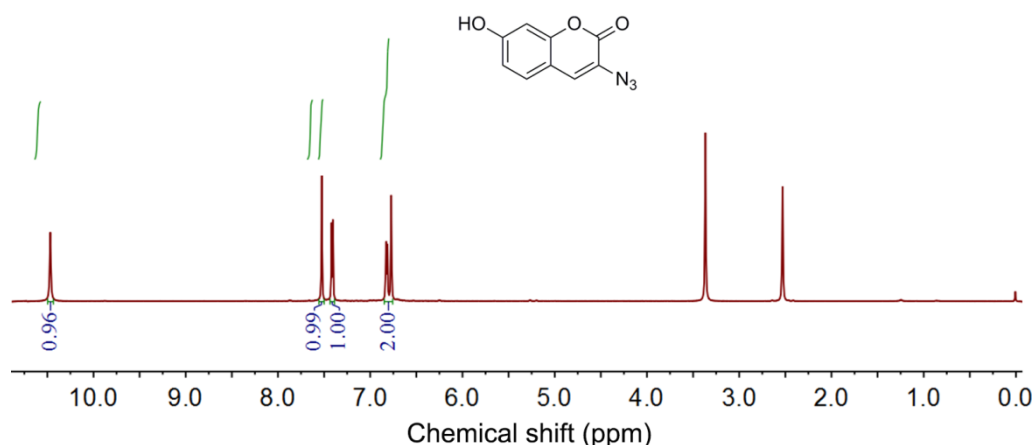
Transmission electron microscopy (TEM) measurements were analyzed on a transmission electron microscope (JEOL JEM-1011). Fourier transform infrared spectroscopy (FTIR) spectra were recorded on a BRUKER Vertex 70 FTIR spectrometer. Nitrogen adsorption-desorption isotherms were recorded on a Micromeritics ASAP 2020M automated sorption analyzer. Flow cytometry was carried out on the flow cytometry (BD LSRFortessa<sup>TM</sup> Cell Analyzer). Inductively

coupled plasma mass spectrometry (ICP-MS) measurements were measured using ICP-MS (ThermoScientific Xseries II).

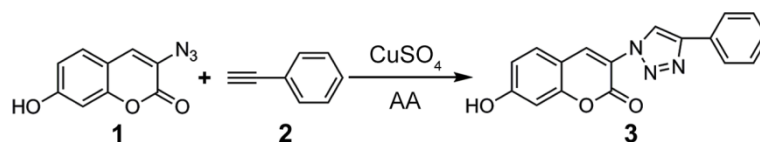
### Synthesis of compound 1



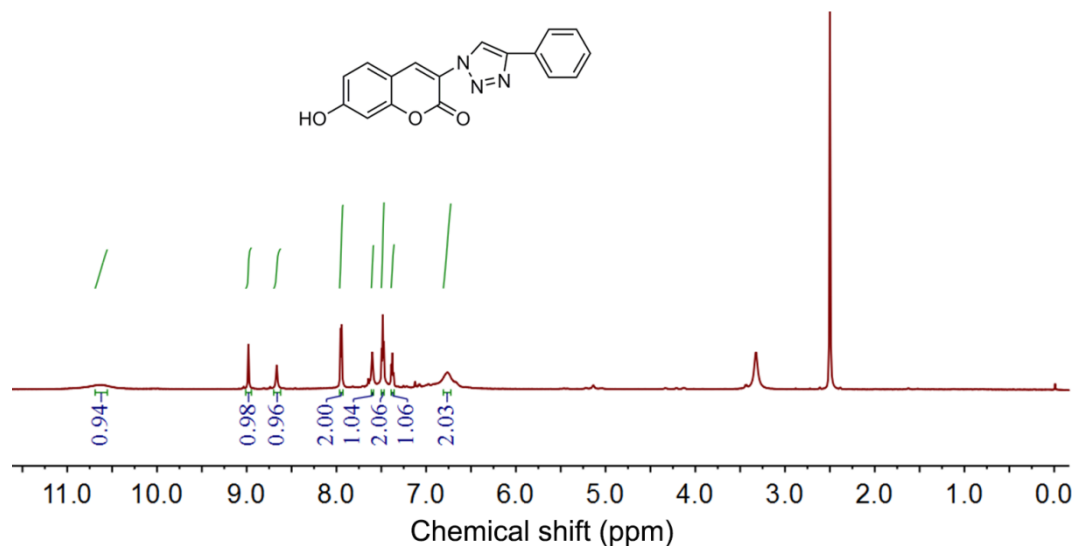
The synthesis followed the literature procedure.<sup>1</sup> A mixture of 2,4-dihydroxy benzaldehyde (10 mmol), *N*-acetylglycine (10 mmol), and anhydrous sodium acetate (30 mmol) in acetic anhydride (50 ml) was refluxed under stirring for 6 h. The reaction mixture was poured onto ice to give a yellow precipitate. After filtration, the yellow solid was washed by ice water before it was refluxed in a solution of concentrated HCl and ethanol (2:1, 15 mL) for 1 h, then ice water (20 mL) was added to dilute the solution. The solution was then cooled in an ice bath and NaNO<sub>2</sub> (20 mmol) was added. The mixture was stirred for 15 min and NaN<sub>3</sub> (30 mmol) was added dropwise. After stirring for 30 min, the resulting precipitate was filtered off, washed with water, and dried under reduced pressure to afford a brown solid (1.04 g, 51%). <sup>1</sup>H NMR (600 MHz, DMSO-*d*<sub>6</sub>)  $\delta$  (ppm): 10.46 (s, 1H), 7.55 (s, 1H), 7.41 (d, *J* = 8.5 Hz, 1H), 6.74-6.85 (m, 2H). MS (ESI) *m/z*: [M-H]<sup>-</sup> calcd for C<sub>9</sub>H<sub>5</sub>N<sub>3</sub>O<sub>3</sub>, 202.2; found 202.2.



### Synthesis of compound 3



Compound **1** (0.5 mmol), **2** (0.5 mmol), CuSO<sub>4</sub> (0.05 mmol) and ascorbic acid (AA, 0.1 mmol) were added to a solution of H<sub>2</sub>O and ethanol (1:1, 10 mL) and stirred at 37 °C for 6 h. Then the ethanol was removed and the residue was extracted with CHCl<sub>3</sub>. Evaporation of the solvent afforded a brown powder. <sup>1</sup>H NMR (600 MHz, DMSO-*d*<sub>6</sub>) δ (ppm): 10.64 (s, 1H), 8.98 (s, 1H), 8.67 (s, 1H), 7.95 (d, *J* = 7.7 Hz, 2H), 7.60 (s, 1H), 7.48 (t, *J* = 7.5 Hz, 2H), 7.37 (d, *J* = 7.5 Hz, 1H), 6.76 (s, 2H). MS (ESI) *m/z*: [M-H]<sup>-</sup> calcd for C<sub>17</sub>H<sub>11</sub>N<sub>3</sub>O<sub>3</sub>: 305.3; found 304.3.



### Synthesis of MSN-NH<sub>2</sub>

Amino-functionalized mesoporous silica nanoparticle (MSN-NH<sub>2</sub>) was prepared according to the procedures with slight modification.<sup>2,3</sup> Briefly, tetraethoxysilane (TEOS, 5 mL), (3-aminopropyl)triethoxysilane (APTES, 1 mL), NaOH (0.28 g), and *N*-cetyltrimethylammonium bromide (CTAB, 1 g) were added to 500 mL water. After stirred at 80 °C for 2 h, the nanoparticles were filtered and washed with water and ethanol. Then the nanoparticles were refluxed in a solution of concentrated HCl and ethanol (1:99, 200 mL) for 8 h to remove CTAB. MSN-NH<sub>2</sub> was separated by centrifuging at 12000 rpm for 10 min.

### **Synthesis of prodrugs-loaded MSN-IgG**

4-carboxyphenylboronic acid (BA, 2 mmol), N-hydroxysuccinimide (NHS, 2 mmol) and 1-[3-(dimethylamino)propyl]-3-ethylcarbodiimide hydrochloride (EDC, 3 mmol) were reacted in DMSO (10 mL) for 1 h. After adding MSN-NH<sub>2</sub> (800 mg), the solution was stirred at room temperature for 12 h and then washed with DMSO to harvest MSN-BA.

Prodrugs-loaded MSN was prepared by a solvent evaporation method.<sup>4</sup> **4** (20 μmol), **5** (20 μmol), AA (20 μmol) and MSN-BA (10 mg) were added to a solution of ethanol and water (1:1, 10 mL). After sonication for 30 min, the solvent was removed slowly in dark. Then prodrugs-loaded MSN-BA was obtained by centrifugation and re-suspended in phosphate buffer saline (PBS). After adding immunoglobulin G (IgG) (20 mg), the solution was stirred in dark for 24 h, following by filtration and washing with PBS. Through the high performance liquid chromatography (HPLC)-based method, the prodrug loading ratios of compound **4**, **5**, and AA for MSN-IgG were measured to be 13.1%, 7.9%, and 10.3%, respectively.

### **AFM studies**

The samples were diluted with deionized water to yield a final concentration of 1 μM. Then aliquots of 60 μL of each sample were placed on a freshly cleaved mica substrate. After incubation for 30 min, the substrate was washed with water and dried before measurement. Tapping mode was used to acquire the images under ambient conditions. The AFM images were processed with Nanoscope software.

### **MALDI-TOF-MS measurements**

After the photo-oxygenation, Aβ solution was added with 10% ethanol and then centrifuged at 13000 rpm for 15 min to remove the HEPES buffer. Then Aβ was re-dissolved in deionized water and stored at 4 °C before the measurement. Sinapic acid was applied as the matrix for MS analysis.

### **Nitrogen adsorption-desorption measurements**

The samples were degassed at 50 °C for 12 h. The specific surface areas were calculated from the adsorption data in the low pressure range using the BET model and pore size was determined following the BJH method.

### **Cell culture**

PC12 cells (rat pheochromocytoma, American Type Culture Collection) were maintained in Dulbecco's minimum essential medium (DMEM, Gibco) supplemented with 5% fetal bovine serum and 10% heat-inactivated horse serum at 37 °C in a humidified atmosphere of 5% CO<sub>2</sub> and 95% air. The media were changed every three days, and the cells were passaged by trypsinization before confluence.

### **Cytotoxicity assays**

Cell viability was measured by 3-(4,5-dimethylthiazol-2-yl)-2,5-diphenyltetrazolium bromide (MTT) assays. PC 12 cells were seeded at a density of 5000 cells/well on 96-well plates for 24 h. Cells were incubated for 24 h after the treatment and then MTT assays were carried out. To determine toxicity, 10 µL of MTT solution was added to each well and the cells were incubated for 4 h. After adding 100 µL DMSO, the absorbance of formazan was read at 490 nm on a SpectraMax M5 microplate reader (Molecular Devices Corp., Sunnyvale, CA, USA). Three replicates were done for each treatment group.

### **Flow cytometry**

PC12 cells were seeded in six-well plates in DMEM for 24 h before further manipulation. Then the cells were treated with as-prepared Aβ-Cu aggregates (10 µM) for 12 h before compound **1** (50 µM), **2** (50 µM), and AA (50 µM) were incubated with cells for another 12 h. The treated cells were washed with PBS twice, and the fluorescence intensity of cells was monitored by flow cytometry (BD LSRFortessa™ Cell Analyzer).

### **Immunocytochemistry**

PC12 cells were treated with 10  $\mu$ M A $\beta$ -Cu aggregates and 20  $\mu$ M compound **6** for 4 h at 37 °C and then washed with PBS. PC12 cells were fixed in 4% paraformaldehyde for 15 min at room temperature (RT). Then, the cells were washed with PBS and blocked with 5% bovine serum albumin (BSA), 0.1% Triton X-100 (in PBS) for 60 min at RT. After washed with PBS, the samples were incubated with mOC78 antibody (diluted 1:1000 in 5% BSA) overnight at 4 °C. Cells were washed with PBS and then incubated with Alexa Fluor 555-labeled anti-mouse IgG secondary antibody (1:200). After washing, cells were observed with fluorescence microscope.

### **ICP-MS measurements**

To investigate whether MSN could access worms' tissues, Si level of MSN-treated worms was detected using ICP-MS (ThermoScientific Xseries II). *C. elegans* was cultured on the NGM containing MSN (1 mg mL<sup>-1</sup>) for 24 h. MSN-treated worms were washed with deionized H<sub>2</sub>O and centrifuged at 1000 rpm thrice. After the worms were lyophilized, worms were lysed with a sonic tip in the ice bath for 15 min. HF (50 wt%, 0.1 mL) and HNO<sub>3</sub> (2 wt%, 9.9 mL) were added to allow dissolution of the silica nanoparticles with ultrasound. The clear acidic solutions were used for ICP-MS analysis.

### **Mouse brain slice culture**

The use of mice followed the guidelines of the Institutional Animal Care and Use Committee. The 3 $\times$ Tg-AD mice were purchased from The Jackson Laboratory (JAX order number 3591206, Bar Harbor, ME, USA), and these mice express the mutant PS1M146V, APP<sup>swe</sup>, and tauP301L transgenes and generally develop A $\beta$  plaques and neurofibrillary tangles that represent the neuropathological process of AD. Twelve-month-old 3 $\times$ Tg-AD or wild-type mice were rapidly sacrificed before further manipulation. Fresh brain tissues were embedded with 3% low melting temperature agarose in artificial cerebrospinal fluid (ACSF), which contained 125 mM NaCl, 5 mM KCl, 1.25 mM NaH<sub>2</sub>PO<sub>4</sub>, 1 mM MgSO<sub>4</sub>, 2 mM CaCl<sub>2</sub>, 25 mM NaHCO<sub>3</sub> and 20 mM D-(+)-glucose. Then the tissues were sectioned into slices with a thickness of 40

µm and temporarily collected in ice-cold ACSF pre-oxygenated with 95% O<sub>2</sub>, 5% CO<sub>2</sub>. After that, the brain slices were transferred onto the slice culture inserts and incubated with culture medium composing of 66% Eagle's basal medium, 25% Hanks balanced salt solution, 5% FBS, 1% N2 supplement, 1% penicillin/streptomycin, 2 mM L-glutamine and 0.66% (w/v) D-(+)-glucose.

### **Statistical analysis**

For the statistical analysis, the experiments were replicated independently. Summary data in figures are presented as mean values and error bars indicate  $\pm$  standard deviation (s.d.).



**Table S1** Cu level in the dialysate after the dialysis experiment.

	A $\beta$ 40-Cu	A $\beta$ 40-Cu + <b>6</b>
Cu in the dialysate/total Cu	0.032 $\pm$ 0.004	0.913 $\pm$ 0.005

For the competition dialysis experiment,<sup>5</sup> A $\beta$ 40-Cu aggregates (10  $\mu$ M) with or without compound **6** (20  $\mu$ M) were dialyzed against deionized water using the molecular porous membrane (retained molecular weight = 2000 Da) at 4 °C for 12 h. The dialysate was concentrated and then mixed with an equal volume of aqua regia to obtain free Cu ion. Cu level in the dialysate was analyzed by ICP-MS. The dialysis experiment revealed compound **6** captured Cu effectively from A $\beta$ 40-Cu aggregates. Each experiment was repeated thrice. Error bars indicate  $\pm$  standard deviation (s.d.).

**Table S2** Normalization of the NR fluorescence intensity of the brain slices from 3 $\times$ Tg-AD mice. The fluorescence intensity at 0 h was defined as 100 %. The semi-quantitative analysis was processed with ImageJ software. Each experiment was repeated thrice. Error bars indicate  $\pm$  s.d.

	light	<b>6</b>	<b>6</b> + light
0 h	100 $\pm$ 2.4	100 $\pm$ 2.3	100 $\pm$ 2.1
12 h	93.2 $\pm$ 2.6	89.3 $\pm$ 3.1	46.1 $\pm$ 3.6

**Table S3** Specific surface value, pore volume, and pore size calculated from nitrogen adsorption-desorption isotherms.

	MSN-NH <sub>2</sub>	MSN-BA	MSN-IgG
specific surface [m <sup>2</sup> g <sup>-1</sup> ]	704.2	653.9	118.1
pore volume [cm <sup>3</sup> g <sup>-1</sup> ]	0.594	0.543	0.158
pore size [nm]	2.93	2.79	—

**Table S4** Si level of MSN-treated cells and untreated cells.

	untreated	MSN-treated
Si level ( $\mu\text{g}/10^6$ cell)	not detected	$62 \pm 5$

PC12 cells were incubated with MSN-IgG ( $0.1 \text{ mg mL}^{-1}$ ) for 24 h, washed with PBS for three times and trypsinized. The cells were suspended in PBS and counted. After lyophilized, the cells were lysed with a sonic tip in the ice bath for 5 min. HF (50 wt%, 0.1 mL) and  $\text{HNO}_3$  (2 wt%, 9.9 mL) were added to allow dissolution of the silica nanoparticles with ultrasound. The clear acidic solutions were used for ICP-MS analysis. Each experiment was repeated thrice. Error bars indicate  $\pm$  s.d.

**Table S5** Si level of MSN-treated worms and untreated worms.

	untreated	MSN-treated
Si level ( $\mu\text{g}/\text{mg}$ worms)	not detected	$8.6 \pm 1.1$

Worms were cultured on the NGM containing MSN ( $1 \text{ mg mL}^{-1}$ ) for 24 h. And then Si level was analyzed by ICP-MS. Each experiment was repeated thrice. Error bars indicate  $\pm$  s.d.

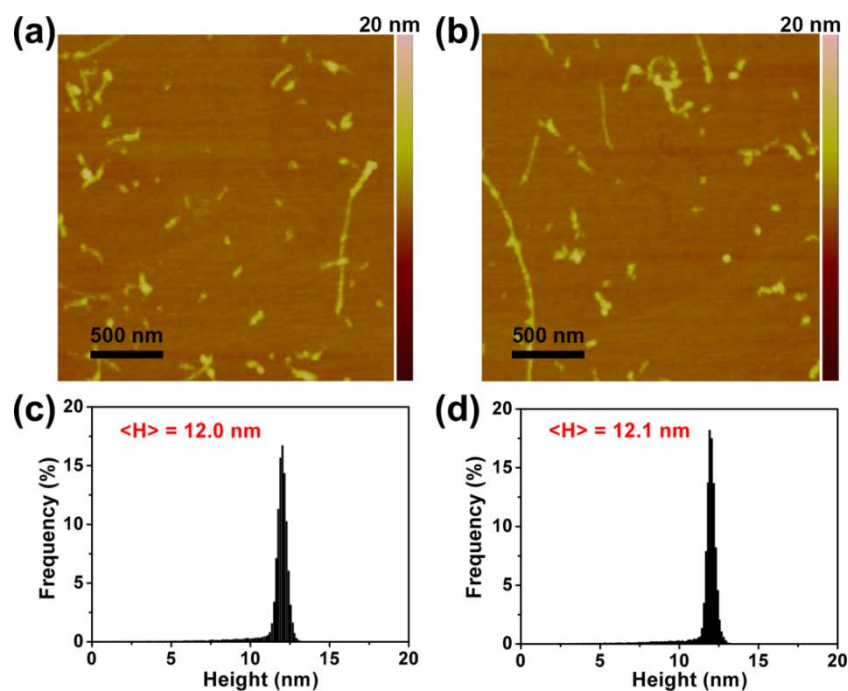


**Fig. S1** Representative AFM images of Aβ40-Cu aggregates before (a) and after (b) the CuAAC reaction. (c) and (d) were the statistical height analysis of (a) and (b), respectively. The mean height was shown as <H>. The morphology of Aβ40-Cu aggregates was well retained after the reaction.

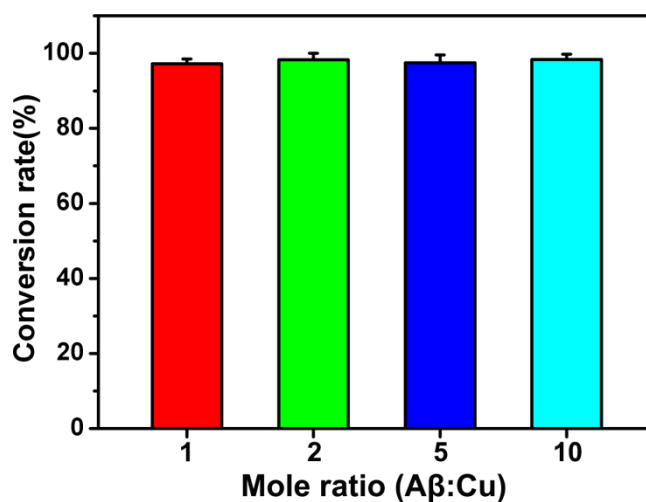


**Fig. S2** Conversion rate of the CuAAC reaction for different ratios of Aβ40 to Cu. Aβ40-Cu species, ascorbic acid (50 μM), compound **1** (50 μM) and **2** (50 μM) were reacted at room temperature for 2 h. The concentration of CuCl<sub>2</sub> was 10 μM. The conversion rate of compound **1** was monitored by <sup>1</sup>H-NMR.

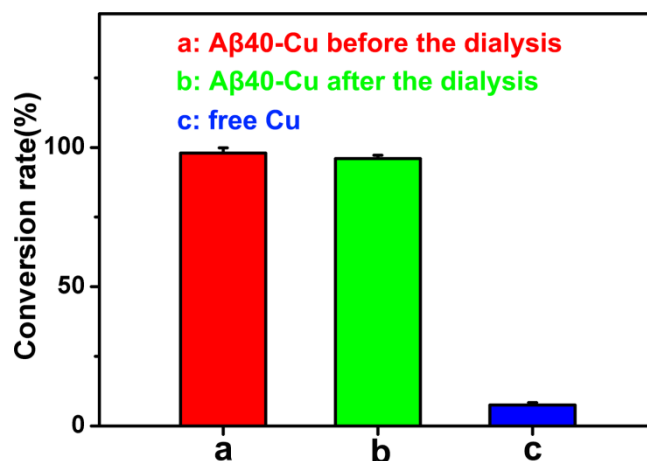


**Fig. S3** Conversion rate of the CuAAC reaction catalyzed by Aβ40-Cu aggregates before and after the dialysis and the free Cu. Cu species (including Aβ40-Cu aggregates before and after the dialysis and the free Cu), ascorbic acid (50 μM), compound **1** (50 μM) and **2** (50 μM) were reacted at room temperature for 2 h. The concentration of Aβ40-Cu aggregates before the dialysis was 10 μM. The conversion rate of compound **1** was monitored by <sup>1</sup>H-NMR. As shown in Fig. S3, the conversion rate didn't show significant difference for Aβ40-Cu aggregates before and after the dialysis. More importantly, free Cu could not efficiently catalyze the CuAAC reaction in 2 h because of very low Cu content (about 0.3 μM).

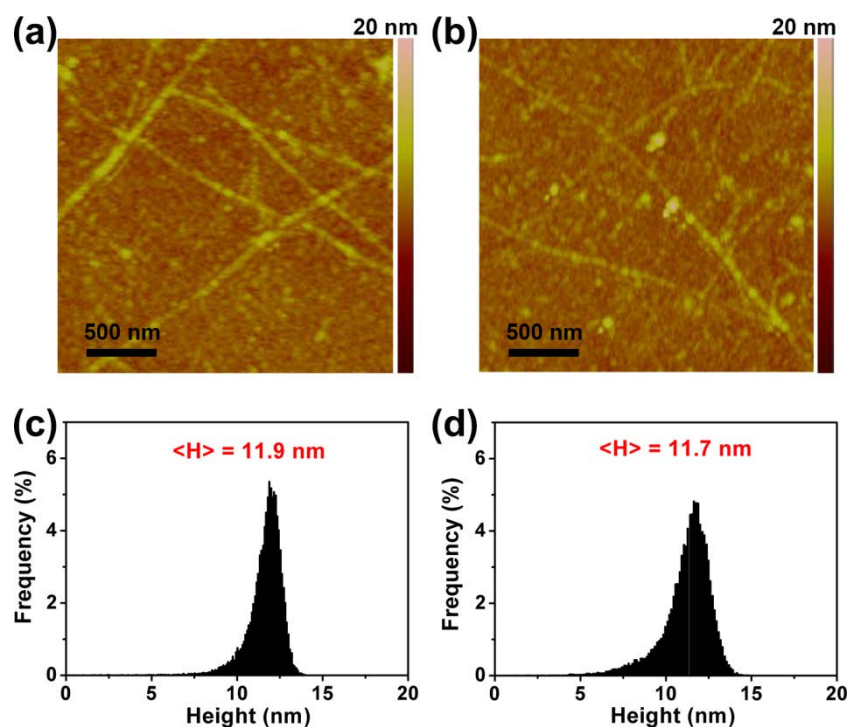


**Fig. S4** Representative AFM images of Aβ42-Cu aggregates before (a) and after (b) the CuAAC reaction. (c) and (d) were the statistical height analysis of (a) and (b), respectively. The mean height was shown as <H>. Statistical height analysis and AFM images demonstrated that Aβ42-Cu aggregates didn't change after the reaction.

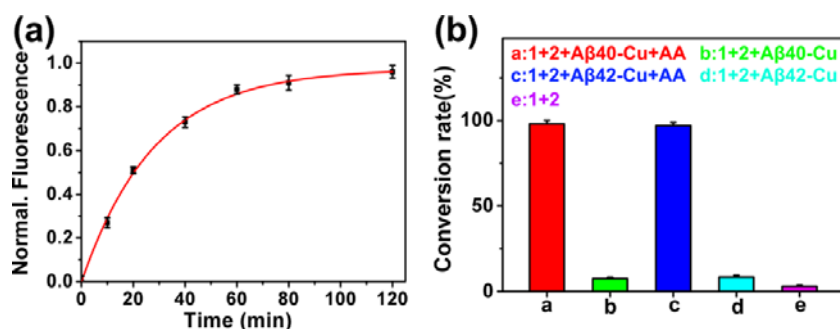


**Fig. S5** (a) Evaluation of the CuAAC reactivity of Aβ42-Cu aggregates using the fluorogenic click reaction. The fluorescence intensity at 475 nm was normalized and the fluorescence intensity of **3** (50 μM) was defined as 100 %. (b) Conversion rate of the CuAAC reaction catalyzed by Aβ40-Cu and Aβ42-Cu aggregates. The conversion rate of compound **1** was monitored by <sup>1</sup>H-NMR. Aβ-Cu aggregates (10 μM), AA (50 μM), compound **1** (50 μM) and **2** (50 μM) were reacted in at room temperature for 120 min. Each experiment was repeated thrice. Error bars indicate ± s.d.

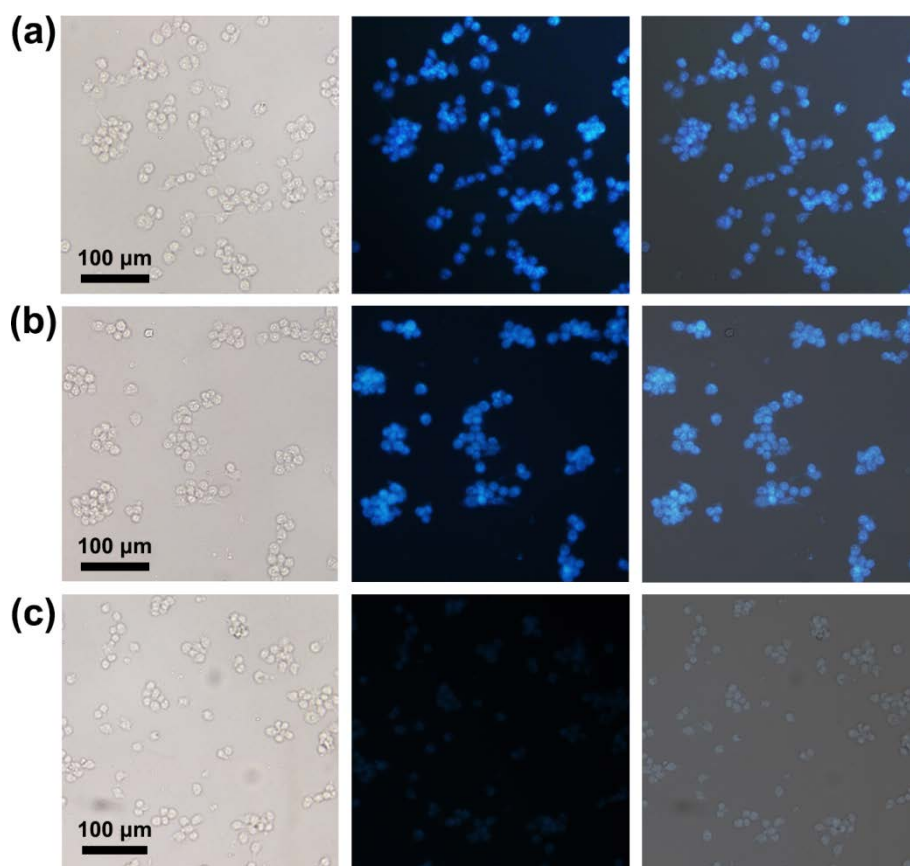


**Fig. S6** The fluorescent microscopy study of intracellular synthesis of compound **3**. PC12 cells were treated with (a)  $\text{CuCl}_2$  or (b)  $\text{A}\beta_{40}\text{-Cu}$  aggregates. (c) Control: untreated cells. Panels from left to right were bright-field, blue channel (synthesized compound **3**), and merged images. Firstly, PC12 cells were treated with  $\text{A}\beta_{40}\text{-Cu}$  aggregates ( $10\ \mu\text{M}$ ) or  $\text{CuCl}_2$  ( $10\ \mu\text{M}$ ) for 12 h and washed with HEPES buffer to remove extracellular Cu species. Then compound **1** ( $50\ \mu\text{M}$ ), **2** ( $50\ \mu\text{M}$ ), and AA ( $50\ \mu\text{M}$ ) were incubated with the cells for another 12 h. As shown in Fig. S6, the click reaction mainly occurred intracellularly.

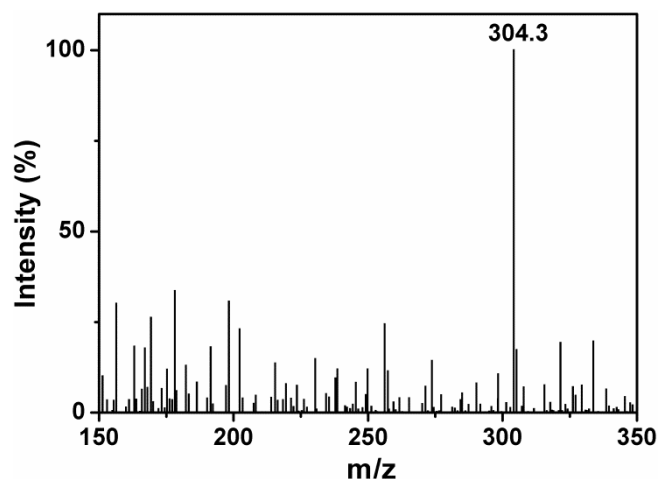


**Fig. S7** MS analysis of the cell lysate, confirming the synthesis of **3** in PC12 cells. After the reaction, the cells were lysed by sonication and the lysate was centrifuged for 5 min at 13000 rpm. The supernatant was mixed with cold acetone and placed under -20 °C overnight. The mixtures were centrifuged for 15 min at 13000 rpm. The solvent was removed under vacuum and the residue was re-dissolved in methanol. The samples were purified by preparative thin-layer chromatography before the MS analysis. 304.3 corresponded to generated compound **3**.

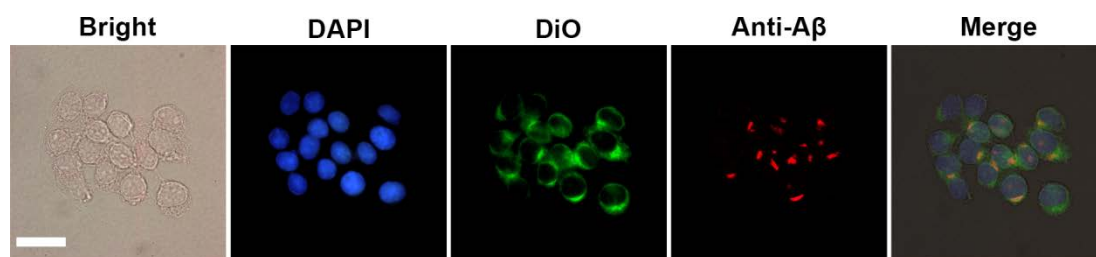


**Fig. S8** Representative fluorescence microscope images. Panels from left to right were bright-field, DAPI (nucleus dye), DiO (cytomembrane dye), A $\beta$  fibril antibody mOC78 and merged images. PC12 cells were incubated with A $\beta$  aggregates for 2 h and washed with HEPES buffer to remove extracellular A $\beta$ 40-Cu. Then the cells were stained with DAPI, DiO and A $\beta$  fibril antibody mOC78. The scale bar is 15  $\mu$ m.

Antibody mOC78 recognizes a conformation-dependent and aggregation-specific discontinuous epitope of A $\beta$  that maps to segments 8-11 (SGYE), 18-24 (VFFAEDV) and 26-32 (SNKGAI).<sup>6</sup>



**Fig. S9** The fluorescent microscopy images of *in situ* synthesized **3** in Cu-treated (a) or normal (b) CL2006 worms. The worms were fixed with 4% paraformaldehyde before taking microscopy images or else worms would move too fast to capture bright-field and fluorescent images at the same location. Panels from left to right were bright-field, blue channel (synthesized compound **3**), and merged images.

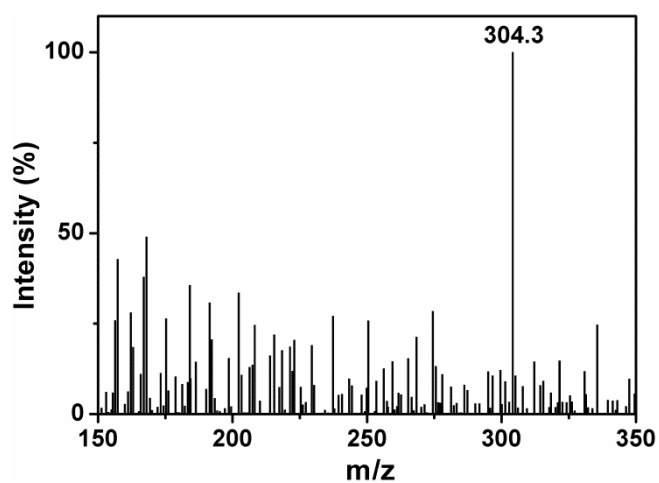


**Fig. S10** MS analysis of the worm lysate, confirming the synthesis of **3** in Cu-treated CL2006 worms.



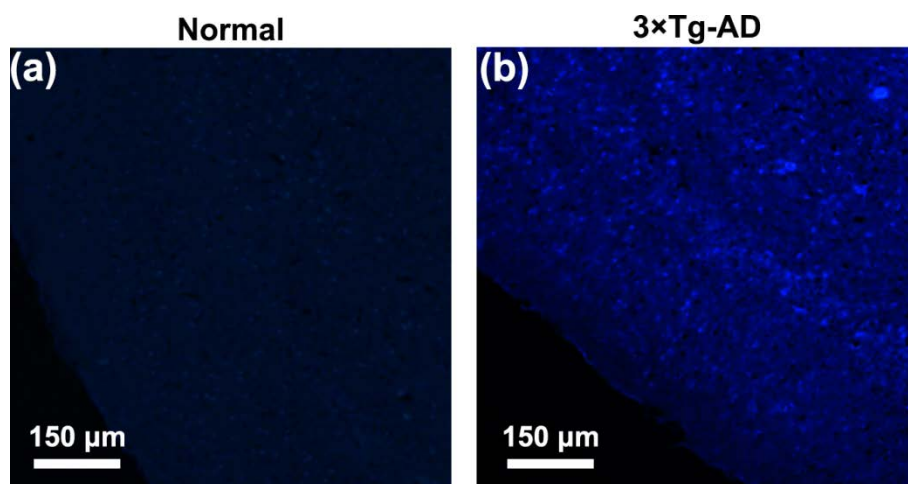


**Fig. S11** The fluorescent microscopy images of *in situ* synthesized compound **3** in the brain slices of normal (a) or 3×Tg-AD (b) mice. The brain slices were incubated with compound **1** (50 μM), **2** (50 μM), and AA (50 μM) for 12 h.

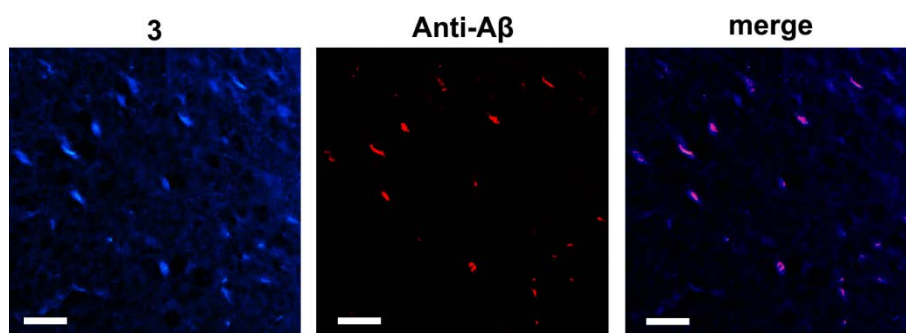


**Fig. S12** Co-location experiment of synthesized compound **3** and Aβ fibrils antibody mOC78 in the brain slices of 3×Tg-AD mice. After the fluorogenic click reaction, the brain slices were stained with antibody mOC78. The scale bar is 100 μm.

As shown in Fig. S12, the fluorescence of compound **3** was intense around Aβ plaques, which meant Aβ-Cu aggregates could catalyze the fluorogenic click reaction in the brain slices. However, due to the diffusion of compound **3**, the fluorophore formation didn't exactly coincide with plaque staining.

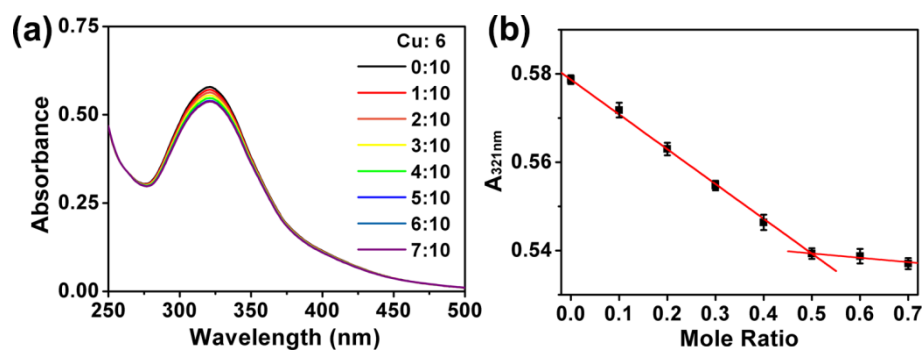


**Fig. S13** (a) UV-vis spectra of compound **6** (20  $\mu\text{M}$ ) titrated by  $\text{Cu}^{2+}$  in HEPES buffer (20 mM, pH 7.4). (b) Absorbance at 321 nm of **6** for different  $\text{Cu}^{2+}$  concentrations. Each experiment was repeated thrice. Error bars indicate  $\pm$  s.d.

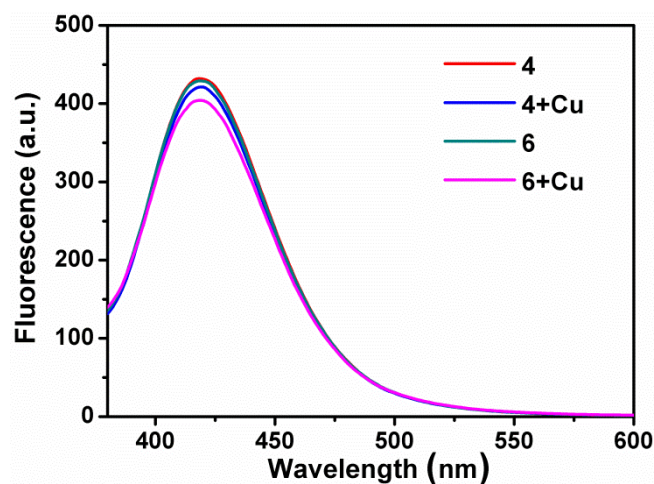


**Fig. S14** Fluorescence spectra of photosensitizers **4** and **6** in the presence or absence of Cu.  $[\mathbf{4}] = 20 \mu\text{M}$ ,  $[\mathbf{6}] = 20 \mu\text{M}$ ,  $[\text{Cu}] = 10 \mu\text{M}$ ,  $\lambda_{\text{ex}} = 335 \text{ nm}$ .

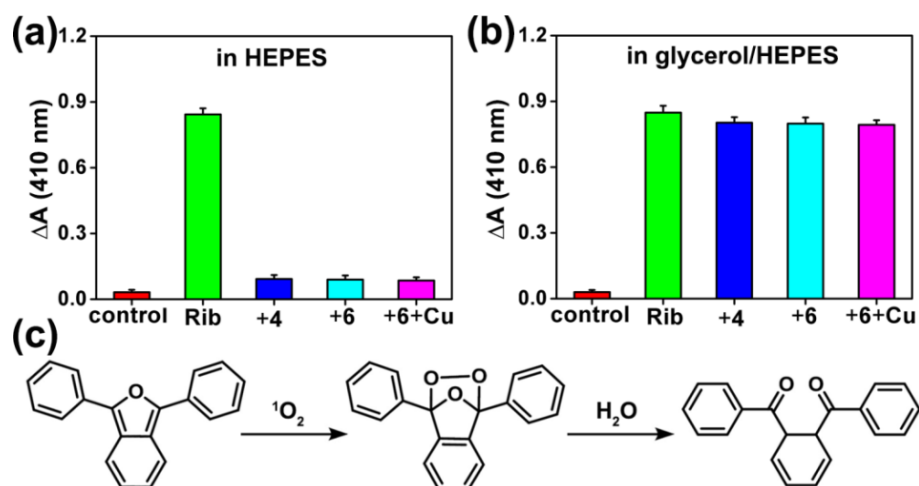


**Fig. S15** (a) Photo-degradation of 1,3-diphenylisobenzofuran (DPBF) treated with compound **4** or **6** or **6** in the presence of Cu in HEPES buffer. Untreated DPBF was used as the control and absorbance decay ( $\Delta A$ ) at 410 nm represented degraded DPBF in 10 min. Riboflavin (Rib), a well-known  $^1O_2$  generator,<sup>7</sup> was used as a positive control. (b) Photo-degradation of DPBF in glycerol/HEPES (7/3, v/v). (c) The degradation mechanism of DPBF. [DPBF] = 50  $\mu M$ , [**4**] = 5  $\mu M$ , [**6**] = 5  $\mu M$ , [Cu] = 2.5  $\mu M$ , [Rib] = 3  $\mu M$ . Each experiment was repeated thrice. Error bars indicate  $\pm$  s.d.

Fig. S15 illustrated that without restricting the bond rotation, photo-excited ThT would undergo twisted intramolecular charge transfer and fail to produce enough ROS.

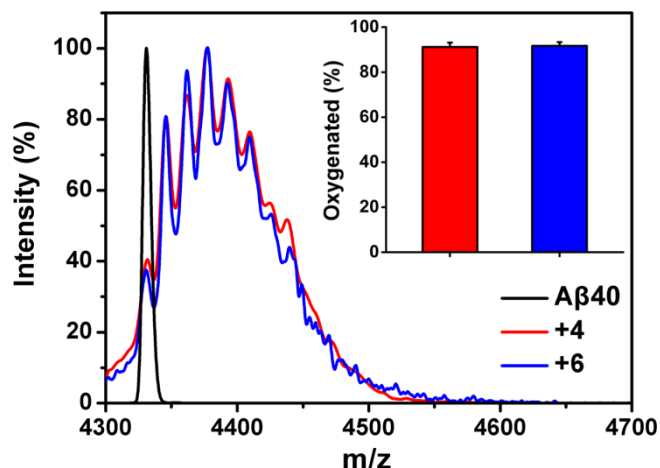


**Fig. S16** MS spectra of A $\beta$ 40 alone and A $\beta$ 40 oxygenated by compound **4** or **6** in the HEPES. The inset shows oxygenated ratio of A $\beta$ 40. The MS peak of native A $\beta$ 40 was 4330 and the MS peaks of oxygenated A $\beta$ 40 were 4346, 4362, 4378, 4394, 4410. Oxygenated ratio (%) = (sum of oxygenated A $\beta$ )/((native A $\beta$ ) + (sum of oxygenated A $\beta$ ))  $\times$  100.<sup>8</sup> Each experiment was repeated thrice. Error bars indicate  $\pm$  s.d.

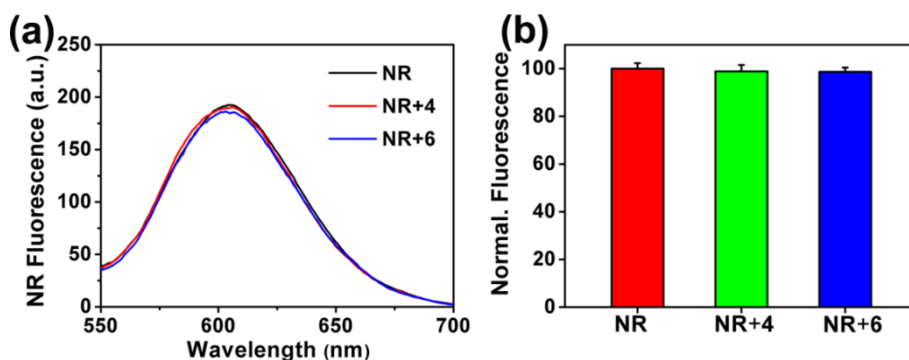


**Fig. S17** (a) Fluorescence spectra of Nile Red (NR) in the presence of compound **4** or **6** ( $\lambda_{\text{ex}} = 530$  nm). (b) Normalized NR fluorescence intensity was corrected for the inner filter effect by the exponential equation  $F_{\text{corr}} = F_{\text{obs}} \times 10^{(A_{\text{ex}} + A_{\text{em}})/2}$ ,<sup>9</sup> where  $F_{\text{corr}}$  and  $F_{\text{obs}}$  were the corrected and observed intensity of fluorescence, respectively, and  $A_{\text{ex}}$  and  $A_{\text{em}}$  were the absorbance at the excitation and emission wavelength, respectively. Each experiment was repeated thrice. Error bars indicate  $\pm$  s.d.

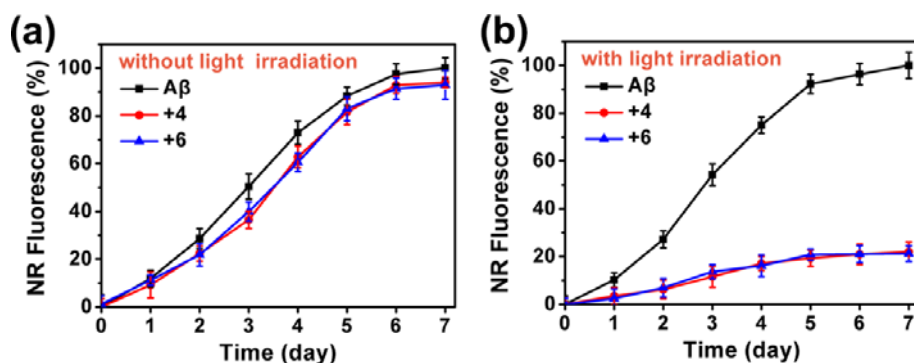


**Fig. S18** Aggregation kinetics of Aβ40 monitored by NR. (a) Aβ40 was incubated in the presence or absence of compound **4** or **6** at 37 °C for 7 days without light irradiation. (b) Aβ40 was irradiated with UV light (1 W cm<sup>-2</sup>) in ice bath for 1 h in the presence or absence of **4** or **6** and then incubated at 37 °C for 7 days. Each experiment was repeated three times. [NR] = 30 μM, [Aβ40] = 10 μM, [**4**] = 20 μM, [**6**] = 20 μM. Each experiment was repeated thrice. Error bars indicate ± s.d.

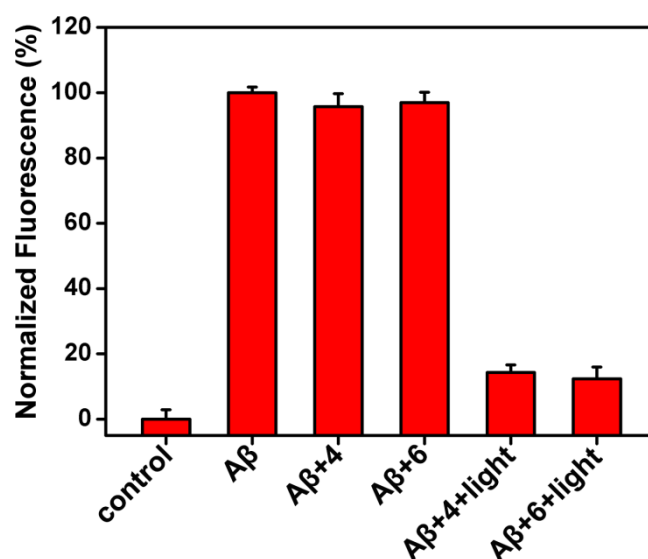


**Fig. S19** Normalized fluorescence of 8-anilinoanthralene-1-sulfonate (ANS) to monitor Aβ40 fibrillation. ANS fluorescence intensity was measured at 470 nm ( $\lambda_{\text{ex}} = 370$  nm). Aβ was irradiated with UV light (1 W cm<sup>-2</sup>) in ice bath for 1 h in the presence or absence of compound **4** or **6** and then incubated at 37 °C for 7 days. Aβ40 monomer was used as the control sample. [ANS] = 30 μM, [Aβ40] = 10 μM, [**4**] = 20 μM, [**6**] = 20 μM. Each experiment was repeated thrice. Error bars indicate ± s.d.

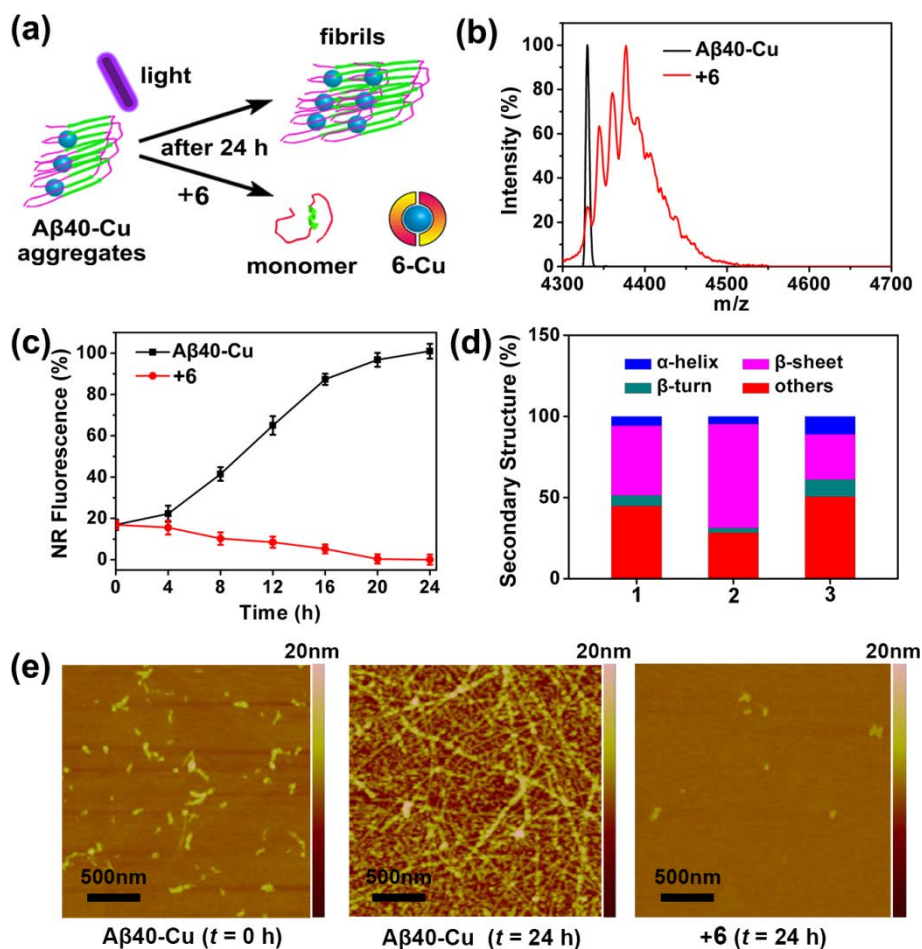


**Fig. S20** Disassembly Aβ40-Cu aggregates with compound **6** under light illumination. (a) Scheme of disaggregating Aβ40-Cu aggregates with **6** though photo-oxidizing Aβ and chelating Cu. (b) MS of Aβ40-Cu aggregates alone or oxygenated by **6**. The oxygenated ratio was about 90.1%. (c) Fibrillation kinetics of Aβ40-Cu aggregates monitored with NR. Each experiment was repeated thrice. Error bars indicate ± s.d. (d) Secondary structure analysis of CD spectroscopy. Column 1: initial Aβ40-Cu aggregates; column 2: Aβ40-Cu aggregates incubated for 24 h; column 3: Aβ40-Cu aggregates incubated with **6** for 24 h. (e) AFM images. Aβ40-Cu aggregates (10 μM) in the presence or absence of **6** (20 μM) were irradiated with UV light (1 W cm<sup>-2</sup>) in ice bath for 1 h. Then the solution was incubated at 37 °C for 24 h.

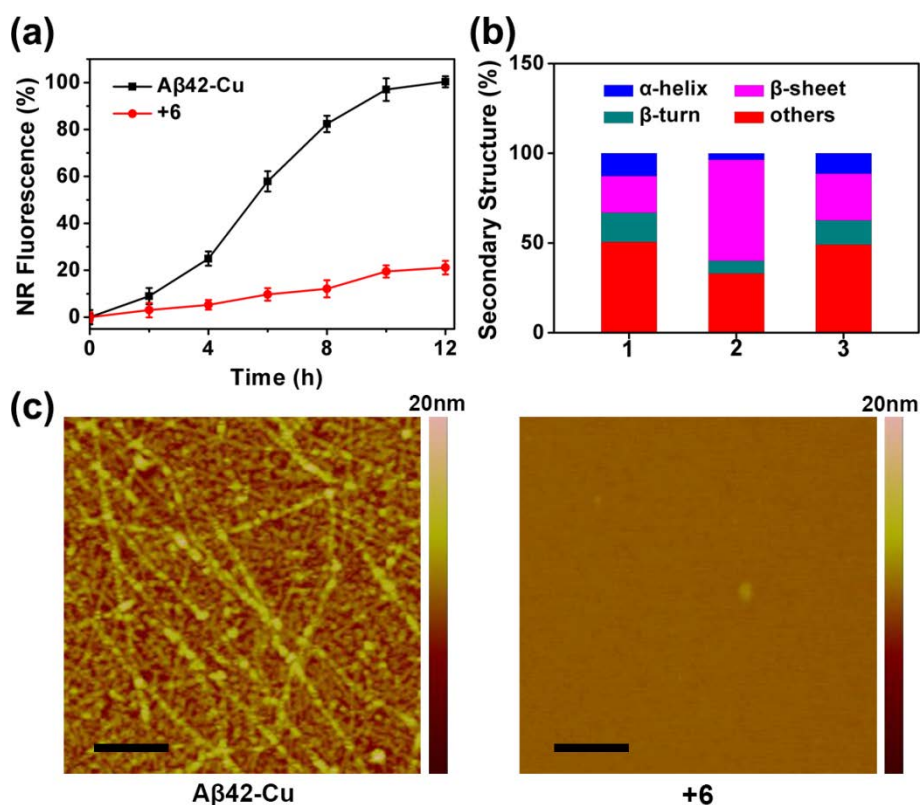


**Fig. S21** Inhibition of Cu-induced Aβ42 aggregation with compound **6** under light illumination. (a) Fibrillation kinetics of Aβ42-Cu alone or in the presence of compound **6**, monitored with NR. Each experiment was repeated thrice. Error bars indicate  $\pm$  s.d. (b) Secondary structure analysis of CD spectroscopy. Column 1: Aβ42 monomer and Cu; column 2: Aβ42-Cu incubated for 12 h; column 3: Aβ42-Cu incubated with **6** for 12 h. (c) AFM images of Aβ42-Cu alone or in the presence of compound **6**. Scale bars: 500 nm. After UV light ( $1 \text{ W cm}^{-2}$ ) irradiating in ice bath for 1 h, Aβ42 monomer ( $10 \mu\text{M}$ ) and Cu ( $10 \mu\text{M}$ ) were incubated with **6** ( $20 \mu\text{M}$ ) for 12 h. Then NR assays, CD spectroscopy, and AFM were conducted to monitor Aβ42 aggregation.



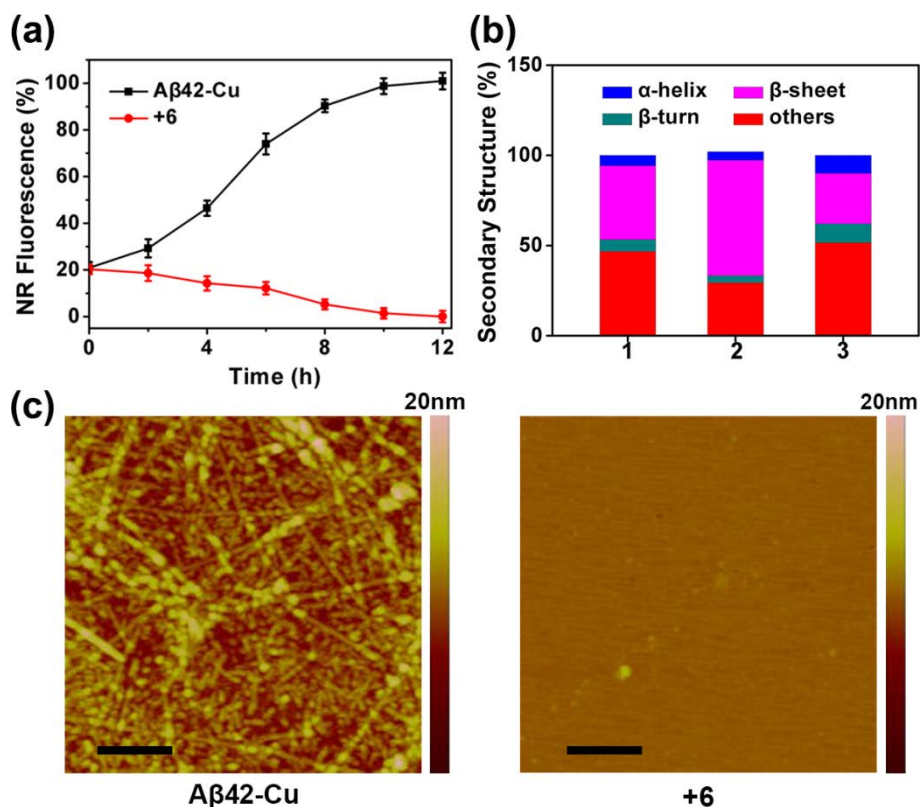


**Fig. S22** Disassembly Aβ42-Cu aggregates with compound **6** under light illumination. (a) Fibrillation kinetics of Aβ42-Cu aggregates monitored with NR. Each experiment was repeated thrice. Error bars indicate  $\pm$  s.d. (b) Secondary structure analysis of CD spectroscopy. Column 1: initial Aβ42-Cu aggregates; column 2: Aβ42-Cu aggregates incubated for 12 h; column 3: Aβ42-Cu aggregates incubated with **6** for 12 h. (c) AFM images of Aβ42-Cu aggregates alone or in the presence of compound **6**. Scale bars: 500 nm. Aβ42-Cu aggregates (10  $\mu$ M) in the presence or absence of **6** (20  $\mu$ M) were irradiated with UV light (1 W cm<sup>-2</sup>) in ice bath for 1 h. Then the solution was incubated at 37 °C for 12 h.



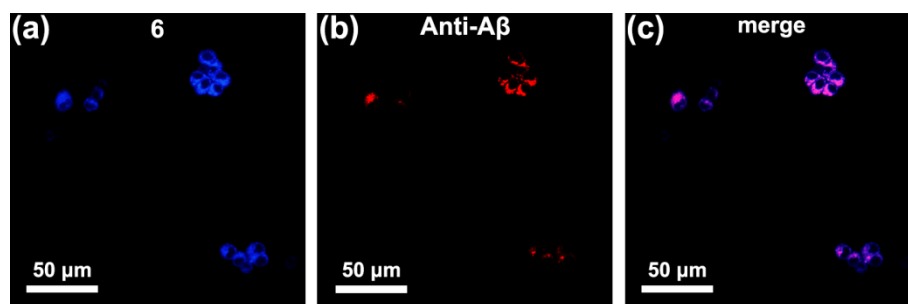


**Fig. S23** Immunofluorescence experiment of compound **6** and A $\beta$  fibrils antibody mOC78 in PC12 cells.

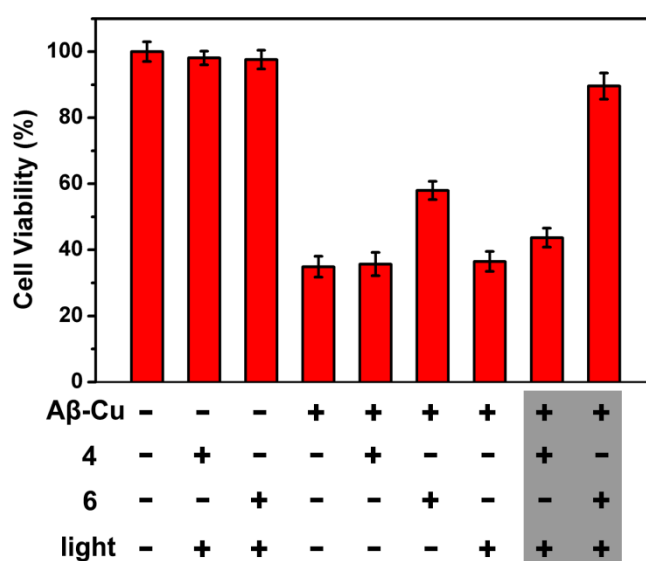


**Fig. S24** MTT assays. A $\beta$ 40-Cu aggregates (10  $\mu$ M) and compound **4** (20  $\mu$ M) or **6** (20  $\mu$ M) were incubated with the cells for 1 h and then irradiated with UV light (1 W  $\text{cm}^{-2}$ ) for 10 min with 20 min interval and for 6 times. Cells were incubated for 24 h and then MTT assays were carried out. Each experiment was repeated thrice. Error bars indicate  $\pm$  s.d. Cellular survival rate didn't decrease obviously for PC12 cells treated with light and **4** or **6** (lane 2 and 3), which confirmed ThT analogues selectively photo-oxygenated  $\beta$ -sheet-rich amyloid aggregates.<sup>8</sup>

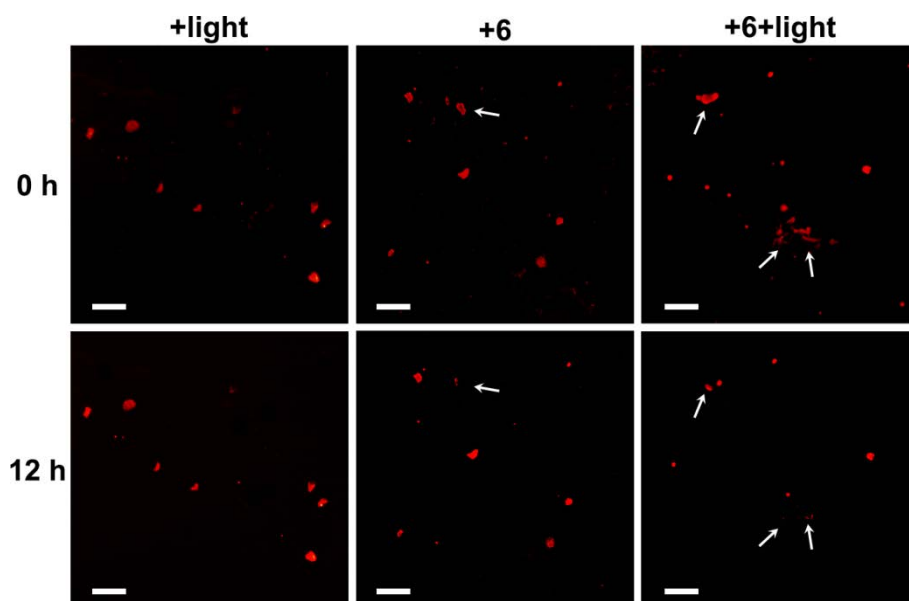


**Fig. S25** Time-lapse imaging of A $\beta$  plaques (white arrows) in the brain slices from 3 $\times$ Tg-AD mice. Firstly, the fresh brain slices were stained with NR (5  $\mu$ M).<sup>10</sup> Then the brain slices were incubated with compound **6** (20  $\mu$ M) and irradiated with UV light (1 W cm<sup>-2</sup>) for 10 min with 20 min interval and for 6 times. Fluorescence images were taken immediately and after 12 h. Scale bars are 100  $\mu$ m.

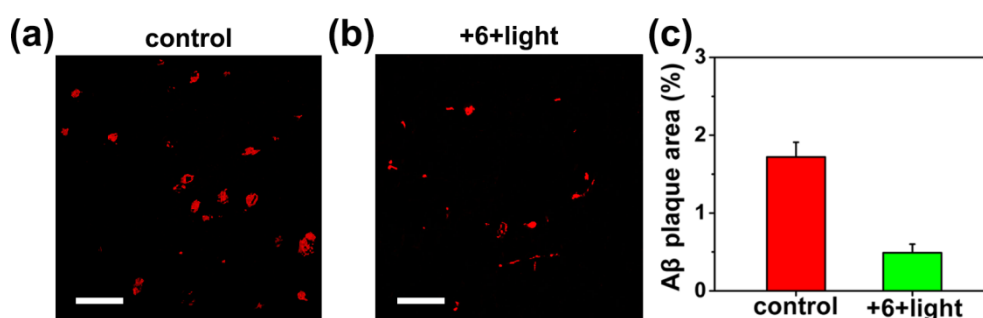


**Fig. S26** Representative images of mOC78 immunoreactive A $\beta$  plaques in the brain slices from 3 $\times$ Tg-AD mice. (a) Control: untreated brain slices. (b) The fresh brain slices were incubated with compound **6** (20  $\mu$ M) and irradiated with UV light (1 W cm<sup>-2</sup>) for 10 min with 20 min interval and for 6 times. After cultured for 12 h, the slices were fixed and coronal sections were cut from frozen slices, followed by immunofluorescent staining with A $\beta$  fibrils antibody mOC78. Scale bars are 100  $\mu$ m. (c) Corresponding quantification of A $\beta$  plaques in hippocampus and cortex.

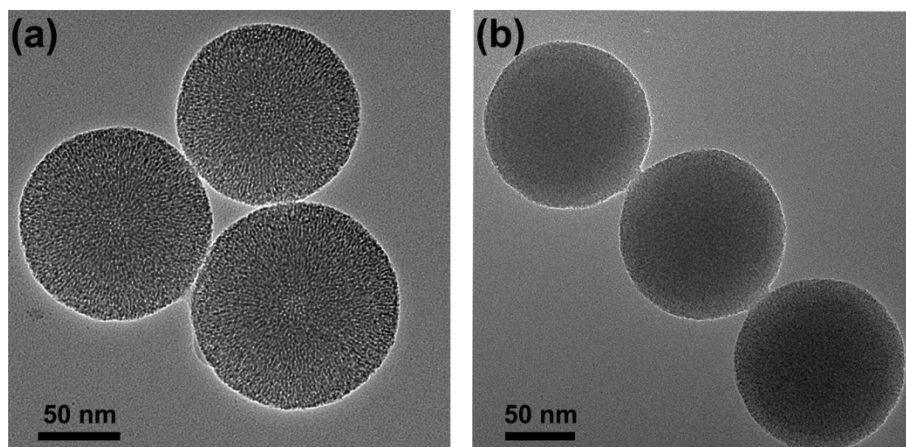


**Fig. S27** TEM images of MSN-NH<sub>2</sub> (a) and MSN-IgG (b). The diameter of MSN was about 120 nm. The hardly detectable mesoporous structure of MSN-IgG indicated that IgG was efficiently immobilized on the MSN.

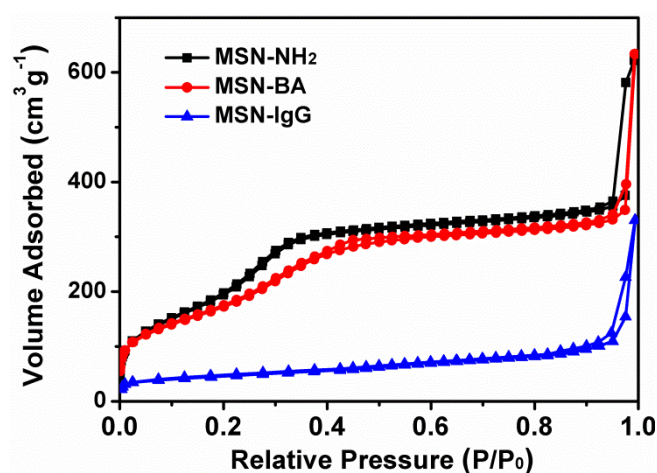


**Fig. S28** Nitrogen adsorption-desorption isotherms of MSN-NH<sub>2</sub>, MSN-BA, and MSN-IgG, which validated IgG was successfully grafting onto the MSN.

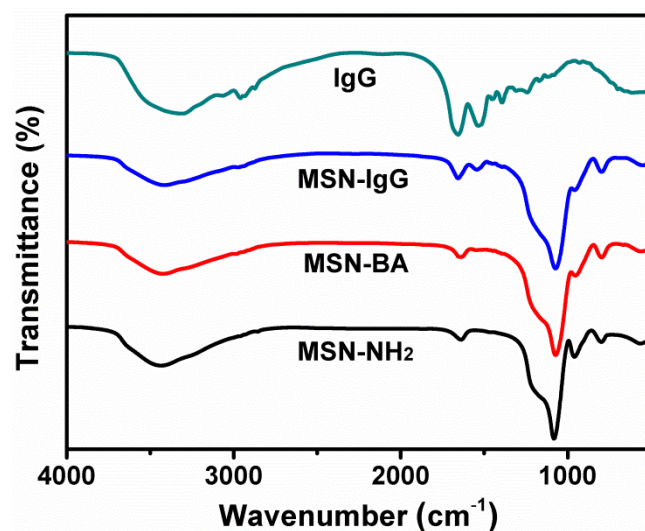


**Fig. S29** FTIR spectra of MSN-NH<sub>2</sub>, MSN-BA, MSN-IgG, and IgG. The typical amide vibration peaks at 1528 cm<sup>-1</sup> and 1649 cm<sup>-1</sup> validated IgG was successfully grafting onto the MSN.

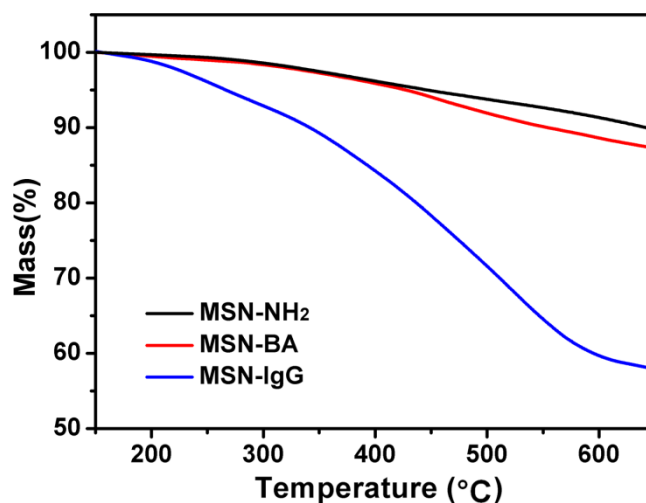


**Fig. S30** Thermogravimetric analysis of MSN-NH<sub>2</sub>, MSN-BA, MSN-IgG. The density of IgG anchored on IgG-MSN was about 2.33 μmol g<sup>-1</sup>.

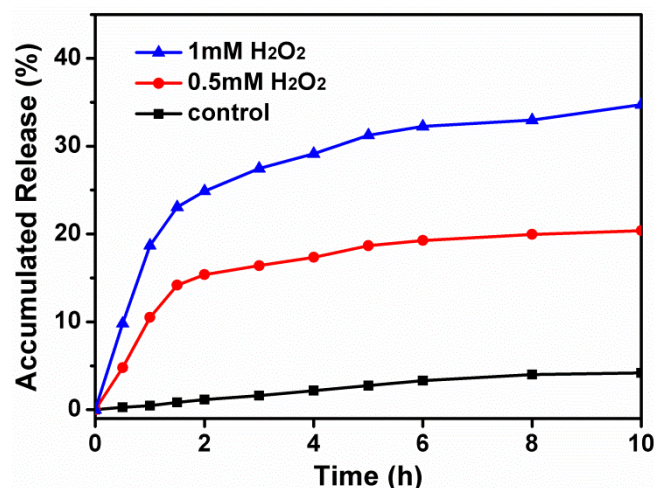


**Fig. S31** Release profiles of compound **4** from MSN-IgG triggered by 0.5 mM or 1 mM H<sub>2</sub>O<sub>2</sub>. The amount of dye release reached about 34.7% within 10 h when MSN-IgG was incubated with 1 mM H<sub>2</sub>O<sub>2</sub>. However, only about 4.2% of **4** was released in the same condition without H<sub>2</sub>O<sub>2</sub>, suggesting that the prodrug was well confined inside the MSN until encountering H<sub>2</sub>O<sub>2</sub>.

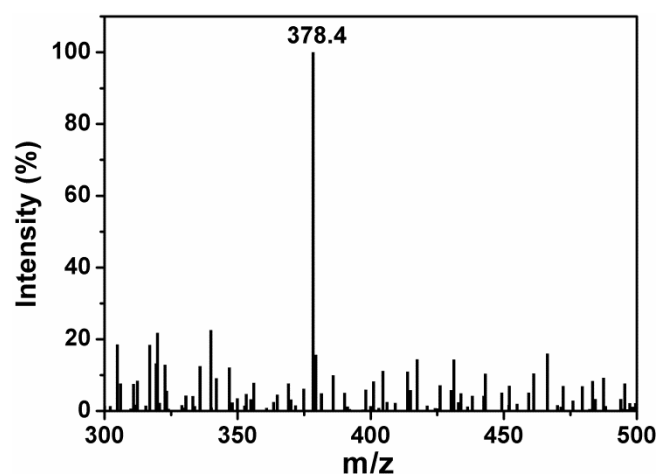


**Fig. S32** MS analysis of the cell lysate, confirming synthesis of compound **6** catalyzed by A $\beta$ -Cu in PC12 cells. A $\beta$ -Cu aggregates (10  $\mu$ M), and prodrugs-loaded MSN-IgG (0.1 mg mL<sup>-1</sup>) were incubated with the cells for 12 h. After the reaction, the cells were lysed by sonication and the lysate was centrifuged for 5 min at 13000 rpm. The supernatant was mixed with cold acetone and placed under -20 °C overnight. The mixtures were centrifuged for 15 min at 13000 rpm. The solvent was removed under vacuum and the residue was re-dissolved in methanol and analyzed by MS. 378.4 corresponded to agent **6**.

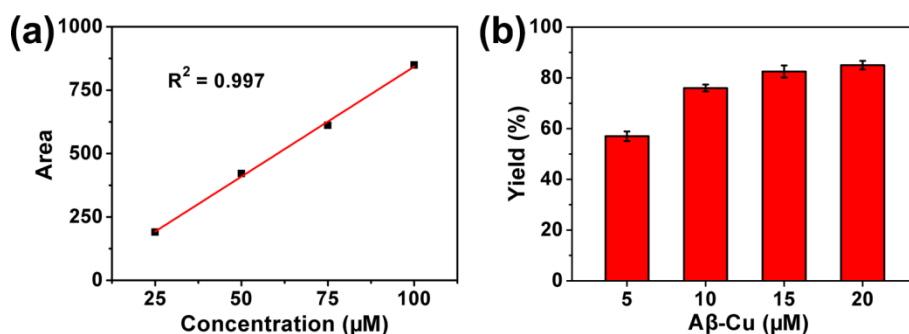


**Fig. S33** LC-MS quantitative analysis of synthesized compound **6**. (a) LC-MS quantitative analysis standard curve of compound **6** by multiple reaction monitoring (MRM). The single quadrupole detector was set for recording only the ion of interest ( $m/z = 378.4$ ). (b) The yield of compound **6** for different Aβ-Cu concentration. The yield was calculated by the loading ratio of compound **4** for MSN-IgG.

PC12 cells were incubated with Aβ40-Cu aggregates of various concentration and prodrugs-loaded MSN-IgG ( $0.1 \text{ mg mL}^{-1}$ ) for 24 h. After the reaction, the cells were lysed by sonication and the cell lysate was lyophilized. The residue was re-dissolved in methanol and quantitatively analyzed by liquid chromatograph mass spectrometer (LC-MS).<sup>11</sup> The LC-MS quantitative analysis was performed using a Waters Acquity UPLC and an autoinjection system hyphenated to a Quattro Premier XE mass spectrometer (Waters, USA) equipped with an electrospray ionization (ESI) source. The separation was achieved using a Thermo AQUASIL C18 column. The system delivered a constant flow of  $250 \text{ μL min}^{-1}$  and the mobile phase was a mixture of methanol and 10 mM ammonium acetate. The volume of injection was 10 μL. As shown in Fig. S33, the yield of compound **6** raised with the increased concentration of Aβ-Cu.

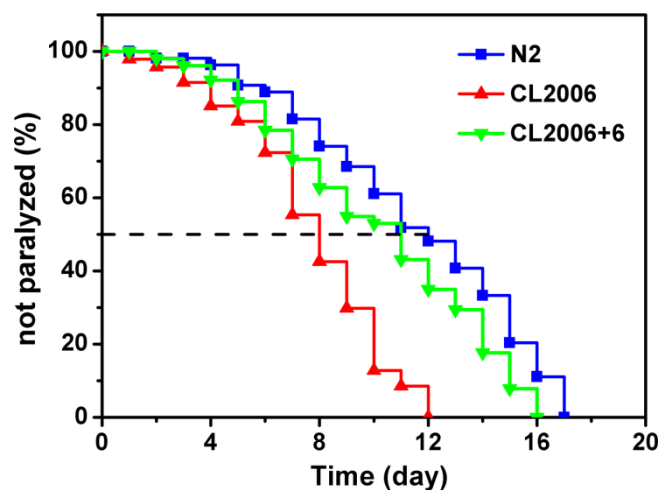


**Fig. S34** Survival curves. Worms were transferred to the NGM containing compound **6** (40  $\mu$ M) for 24 h before worms were irradiated with UV light (1 W  $\text{cm}^{-2}$ ) for 10 min with 20 min interval and for 6 times. The wild-type N2 strain and untreated CL2006 were used as the control. Each experiment was repeated thrice. Error bars indicate  $\pm$  s.d.

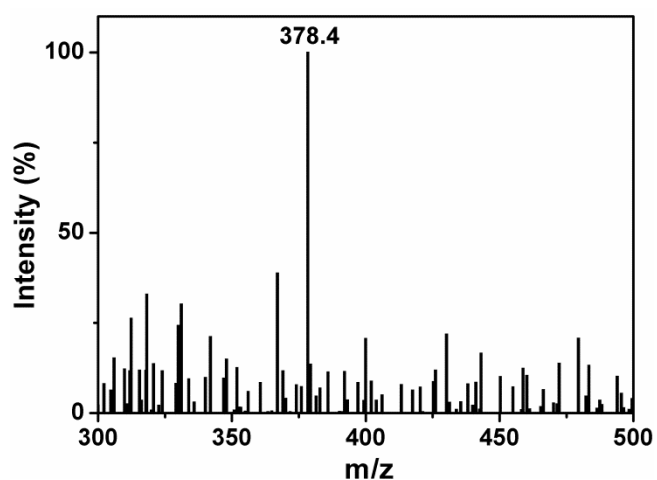


**Fig. S35** MS analysis of the worm lysate, confirming synthesis of compound **6** in Cu-treated CL2006 worms.

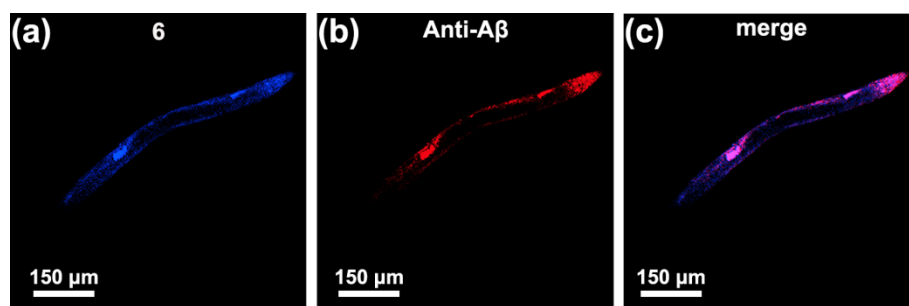


**Fig. S36.** Immunofluorescence experiments for compound **6** and A $\beta$  fibrils antibody mOC78 in CL2006 strain.



## References

- 1 K. Sivakumar, F. Xie, B. M. Cash, S. Long, H. N. Barnhill and Q. Wang, *Org. Lett.*, 2004, **6**, 4603-4606.
- 2 Z. Chen, Z. Li, Y. Lin, M. Yin, J. Ren and X. Qu, *Biomaterials*, 2013, **34**, 1364-1371;
- 3 J. Geng, M. Li, L. Wu, C. Chen and X. Qu, *Adv. Healthcare Mater.*, 2012, **1**, 332-336.
- 4 M. Ren, Z. Han, J. Li, G. Feng and S. Ouyang, *Mater. Sci. Eng. C*, 2015, **56**, 348-355.
- 5 Z. Du, Y. Guan, C. Ding, N. Gao, J. Ren and X. Qu, *Nano Research*, 2018, **11**, 4102-4110.
- 6 A. Hatami, R. Albay, S. Monjazebe, S. Milton and C. Glabe, *J. Biol. Chem.*, 2014, **289**, 32131-32143.
- 7 A. Taniguchi, D. Sasaki, A. Shiohara, T. Iwatsubo, T. Tomita, Y. Sohma and M. Kanai, *Angew. Chem. Int. Ed.*, 2014, **53**, 1382-1385.
- 8 A. Taniguchi, Y. Shimizu, K. Oisaki, Y. Sohma, M. Kanai, *Nat. Chem.*, 2016, **8**, 974-982.
- 9 M. M. Lurtz and S. E. Pedersen, *Mol. Pharmacol.*, 1999, **55**, 159-167.
- 10 H. Sun, J. Liu, S. Li, L. Zhou, J. Wang, L. Liu, F. Lv, Q. Gu, B. Hu, Y. Ma and S. Wang, *Angew. Chem. Int. Ed.*, 2019, **58**, 5988-5993.
- 11 J. Wang, B. Cheng, J. Li, Z. Zhang, W. Hong, X. Chen and P. R. Chen, *Angew. Chem. Int. Ed.* 2015, **54**, 5364-5368.